

Hot electrons and curves of constant gain in long wavelength quantum well lasers

Vera Gorfinkel, Mikhail Kisin and Serge Luryi

Electrical Engineering Department

State University of New York at Stony Brook

Stony Brook, NY 11794-2350

Serge@ee.sunysb.edu

Abstract: In long wavelength quantum well lasers the effective electron temperature (T_e) is often a strong function of the pump current and hence the T_e correlates with the carrier concentration n in the active region. On the other hand, the material gain g in the active layer depends on both variables, $g=g(n, T_e)$. We discuss a convenient way of analyzing this situation, based on considering the contours of constant gain g on the surface $g(n, T_e)$. This is qualitatively illustrated with two model examples involving quantum well lasers, the long-wavelength quantum well laser with current dominated by the Auger recombination and the unipolar quantum cascade laser.

©1998 Optical Society of America

OCIS codes: (140.5960) Semiconductor lasers; (230.5590) Quantum-well devices

References and links

1. S. Luryi, "Hot electrons in semiconductor devices", in *Hot Electrons in Semiconductors*, N. Balkan, ed. (Oxford University Press, 1998) pp. 385-427; <http://www.ee.sunysb.edu/~serge/152.dir/152.html>
 2. V. B. Gorfinkel and S. Luryi, "Fundamental limits for linearity of CATV lasers", *J. Lightwave Technol.* **13**, 252-260 (1995); <http://www.ee.sunysb.edu/~serge/133.html>
 3. M. Silver, E. P. O'Reilly, and A. R. Adams, "Determination of the wavelength dependence of Auger recombination in long-wavelength quantum-well semiconductor lasers using hydrostatic pressure", *IEEE J. Quantum Electron.* **33**, 1557-1566 (1997).
 4. Z. Shi, M. Tacke, A. Lambrecht, and H. Böttner, "Midinfrared lead salt multi-quantum-well diode lasers with 282 K operation", *Appl. Phys. Lett.* **66**, 2537-2539 (1995).
 5. H. K. Choi, G. W. Turner, and H. Q. Le, "InAsSb/InAlAs strained quantum-well lasers emitting at 4.5 μm ", *Appl. Phys. Lett.* **66**, 3543-3545 (1995).
 6. J. R. Meyer, I. Vurgaftman, R. Q. Yang, and L. R. Ram-Mohan, "Type-II and Type-I interband cascade lasers", *Electron Lett.* **32**, 45-46 (1996).
 7. J. Faist, F. Capasso, C. Sirtori, D. L. Sivco, J. N. Baillargeon, A. L. Hutchinson, S.-N. G. Chu, and A. Y. Cho, "High power mid-infrared ($\lambda \sim 5\mu\text{m}$) quantum cascade lasers operating above room temperature", *Appl. Phys. Lett.* **68**, 3680-3682 (1996).
 8. Vera Gorfinkel, Serge Luryi, and Boris Gelmont, "Theory of gain spectra for quantum cascade lasers and temperature dependence of their characteristics at low and moderate carrier concentrations", *IEEE J. Quantum Electron.* **32**, 1995-2003 (1996); <http://www.ee.sunysb.edu/~serge/145.html>
 9. M. V. Kisin, V. B. Gorfinkel, M. A. Stroschio, G. Belenky, and S. Luryi, "Influence of complex phonon spectra on intersubband optical gain", *J. Appl. Phys.* **82**, 2031-2038 (1997); <http://www.ee.sunysb.edu/~serge/148.pdf>
-

1. Introduction

Hot electron effects [1] enter the description of the semiconductor laser operation owing to the dependence of the optical gain g on the carrier temperature T_e . In near infrared lasers, hot electron effects are relatively small and arise mainly from heterostructure barrier injection and free-carrier absorption of cavity radiation. Nevertheless, even these small effects are not entirely benign: they are responsible for a substantial intermodulation distortion limiting the number of channels in optical communication systems [2].

Hot electron effects are more dramatic in longer wavelength materials. This happens because of the substantial release of power that accompanies non-radiative recombination. An important component of the non-radiative current in all long-wave materials is owing to Auger recombination. Recently, Silver *et al.* estimated [3] that Auger processes give a dominant current contribution already at communication wavelengths, 1.75-1.3 μm . Correct account of the Auger contribution become progressively more critical at longer wavelengths, especially in the mid-infrared region [4-6].

In every Auger recombination event, the potential energy of an electron and hole pair (which exceeds the semiconductor energy gap) is transferred to a free electron or hole. At high injection current I , this may lead to a substantial carrier heating. The increased carrier temperature T_e suppresses the optical gain g and may even lead to the appearance of a maximum g_{max} in the dependence $g(I)$. If the total losses in the laser cavity exceed g_{max} then the structure will not lase at any current. Note that for a constant T_e , the "isotherm" dependence $g(I)$ is always monotonic. If the losses do not exceed g_{max} , then the generation regime can be reached, but the negative slope of the $g(I)$ characteristic may result in peculiar instabilities for currents exceeding $I_{\text{cr}}=I(g_{\text{max}})$. For the same value of gain one would have two regimes that differ in the carrier concentration and the temperature and, of course, in the output radiation power. The higher T_e regime would correspond to higher concentration and lower power. Such a regime should be metastable. It could be switched into the stable lower- T_e regime by a sufficiently powerful external illumination pulse that would temporarily suppress Auger recombination processes.

Analogous phenomena can be expected in the operation of unipolar cascade lasers (QCL) at high enough temperatures [7]. Instead of Auger processes, carrier heating in the QCL results from non-radiative intersubband transitions. Again, a kinetic energy on the order of the lasing photon energy is transferred to the electronic system in every transition. The dependence of gain on T_e arises owing to the de-phasing of inter-subband transition by scattering processes whose rate depends on the electron energy and also from the non-parabolicity of the conduction band. The resultant non-monotonic $g(I)$ is responsible [8] for the strong temperature dependence of the QCL threshold with an abrupt disappearance of lasing above a critical temperature.

The purpose of this work is to discuss a simple though powerful approach to such phenomena. It is based on the consideration of curves of constant modal gain,

$$g(n, T_e) = \alpha. \quad (1)$$

Equation (1) defines a family of curves $T_e(n)$. These curves, referred to below as "isogains", provide a "phase portrait" of the laser. For a given value of the total loss α , the intersection of a corresponding isogain with the $T_e(n)$ curve that results from the energy balance equation, defines the operating point of the laser. If for a particular α there is no intersection, such a device will not generate at any pumping.

2. Examples

2.1 Quantum-well laser with Auger heating

The laser operation is modeled by the standard rate equations together with an energy balance equation, where the input power includes the Auger recombination term $E_{\text{eff}} C_A n^3$, where E_{eff} is an effective energy transferred into the carrier system per each act of pair recombination:

$$\frac{nk(T_e - T)}{\tau_E} = E_{\text{eff}} C_A n^3 . \quad (2)$$

The modal gain is taken in the form appropriate for optical transitions at the fundamental absorption edge in the quantum well, viz.

$$g(n, T_e) = \Gamma g_0 (1 - f_e - f_h) , \quad (3)$$

where f_e and f_h are the Fermi functions, describing the occupation of electrons and holes, respectively, at the bottom of the quantum well, viz.

$$f_e(n, T_e) = 1 - e^{-\frac{\pi \hbar^2 n}{m_e k T_e}} \quad (4a)$$

$$f_h(n, T_e) = 1 - e^{-\frac{\pi \hbar^2 n}{m_h k T_e}} \quad (4b)$$

Figure 1 shows the two-parameter surface describing the dependence of gain (3) on both the carrier concentration and temperature. The assumed parameters are indicated in the caption.

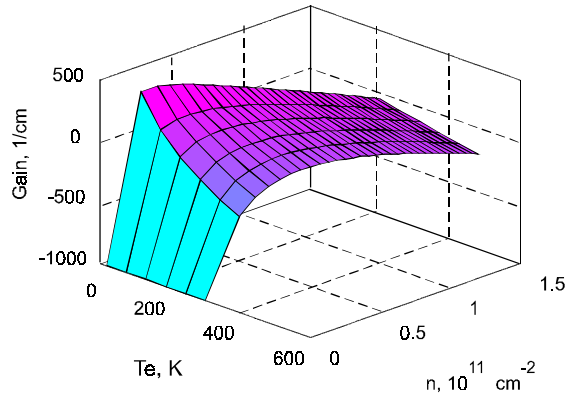


Figure 1. Dependence of the modal gain (3) on the carrier concentration n and temperature T_e . Device comprises $N=10$ quantum wells of width 15 nm, $g_0 = 10^3 \text{ cm}^{-1}$, the mode confinement factor $\Gamma=0.01N=0.1$, the effective energy transferred per carrier pair $E_{\text{eff}} = 1.5E_G + \Delta E_G = 0.75 \text{ eV}$, where $E_G=0.3\text{eV}$ is the bandgap in the active region and $\Delta E_G=0.3\text{eV}$ is the band discontinuity between the active region and the cladding; the energy relaxation time $\tau_e=10^{-12}\text{s}$, the Auger coefficient $C_A=10^{-26} \text{ cm}^6/\text{s}$, and the effective carrier masses are $m_e=0.025 m_0$ and $m_h=20 m_e$.

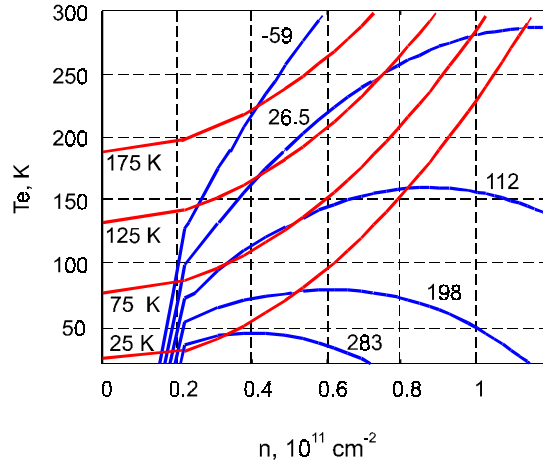


Figure 2. The contours of constant gain for the $g(n, T_e)$ of Fig.1. The isogain curves are shown in blue color for selected values of modal gain $g = \alpha$ indicated in units of cm^{-1} . Red curves show the relation between T_e and n from the energy balance (2).

The contours of constant gain of the 2D surface $g(n, T_e)$ are the isogain curves we are interested in. These curves are shown in Fig. 2 in blue color with each isogain labeled by the value of α in cm^{-1} . The red curves in Fig. 2 show the relation between T_e and n that results from the energy balance (2). The intersection between these curves and an isogain $g = \alpha$ determines the generation point for given loss α . Thus, for $\alpha = 112 \text{ cm}^{-1}$ there is a robust generation region at $T = 25 \text{ K}$ while for $T = 75 \text{ K}$ the generation condition is barely reachable; for $T = 125 \text{ K}$ and $\alpha = 112 \text{ cm}^{-1}$ the lasing regime cannot be reached.

2.2 Quantum cascade laser

The QCL model used is described in Ref. [8]. The energy balance equation is of the form

$$\frac{nk(T_e - T)}{\tau_\varepsilon} = \frac{n_2}{\tau_{21}} \quad (5)$$

where n is the total sheet carrier concentration in both subbands, n_2 is the electron concentration in the upper subband, and τ_{21} is the intersubband transition rate. The latter depends on the carrier temperature, being mainly determined by the emission of polar optic phonons. Equation (5) assumes that all carriers in each cascade period of the QCL have the same temperature, which is a reasonable approximation if n is not too low [8]. The value of τ_{21} affects the QCL operation not only through the energy balance (5) but primarily because it controls the subband population ratio,

$$\frac{n_1}{n_2} = \frac{\tau_{1out}}{\tau_{21}} \quad (6)$$

The dependence $\tau_{21} = \tau_{21}(T_e)$ was calculated in our earlier work [9] and is shown in Fig.3. The value of τ_{1out} describing the escape of electrons from the quantum well was assumed independent of the carrier temperature and equal 0.5 ps.

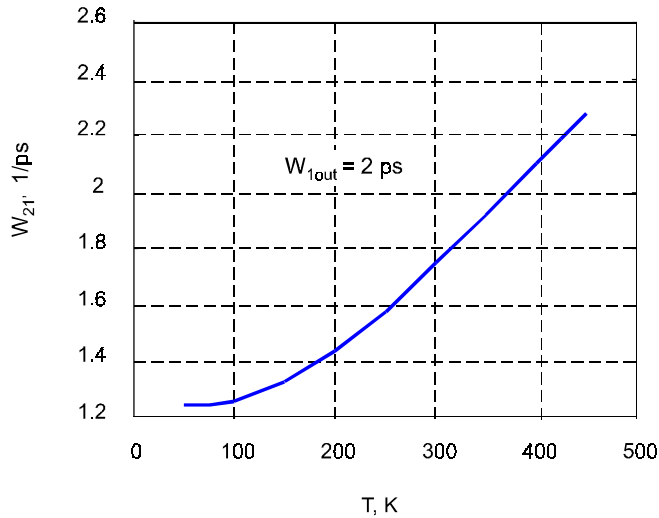


Figure 3. Temperature dependence of the intersubband transition rate in a model quantum cascade laser.

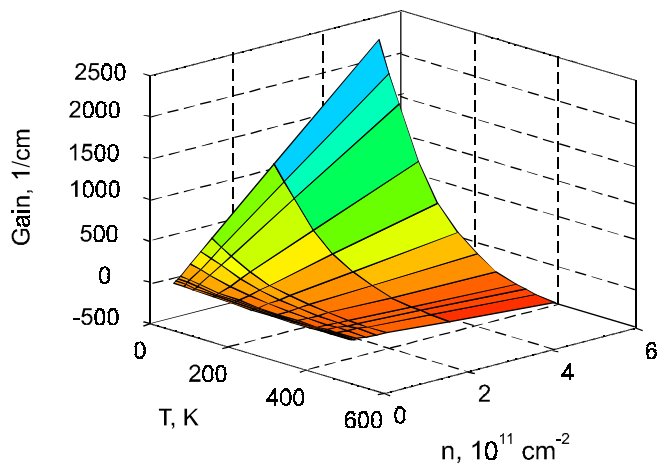


Figure 4. The 2D surface $g(n, T_e)$ for a model quantum cascade laser.

The 2D surface $g(n, T_e)$ calculated in the model [8,9] of intersubband transitions is shown in Fig.4. The model assumes a quasi-equilibrium distribution of electrons in each of the two subbands, characterized by the same effective temperature. The population ratio between the subbands is given by (6). The contours of constant gain $g=\alpha$, corresponding to the surface $g(n, T_e)$ are plotted in Fig. 5 in blue with the values of α indicated. The red lines correspond to the T_e versus n relation as given by the energy balance equation (5). Evidently, in the present model the temperature does not vary with the overall concentration $n=n_1+n_2$ so long as the ratio n_1/n_2 is fixed and that depends on temperature only.

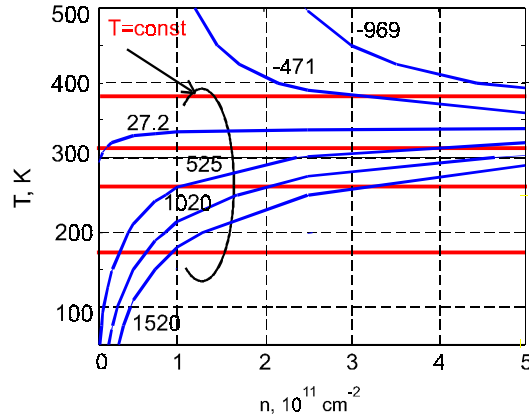


Figure 5. The contours of constant gain (blue) for the $g(n, T_e)$ surface of Fig.4. Red lines indicate the carrier temperature as fixed by equations (5) and (6). In the present model of carrier heating the carrier temperature T_e is independent of n .

The shape of isogain curves in Fig.5 reflects the fact that the sign of g in this model is fixed by the ratio of subband concentrations. If the gain is positive, it increases with n , if it is negative it decreases with n . Evidently, at the transparency value, which is attained when $n_1 = n_2$, i.e., at the temperature when $\tau_{21}(T_e) = \tau_{1out}$, the gain is independent of the overall sheet carrier density in the quantum well.

Conclusion.

We have illustrated a powerful and convenient way of analyzing the situation when the optical gain in a semiconductor laser is a strong function of a parameter other than the carrier concentration. An example (but by no means the only example) of such a parameter is the effective carrier temperature, which has a strong influence on the operation of all long wavelength quantum well lasers. The phase portrait of the laser gain function, represented by the “isogain” contours $g=a$ on the surface $g(n, T_e)$ contains valuable information and offers a unique view of the highly nonlinear device.

Acknowledgement.

This work was supported by the U.S. Army Research Office under grant DAAG55-97-1-0009